applied mechanics

MDPI

Article

Accelerated Carbonation for Improving Mechanical Performance of Sustainable Fiber-Cements Containing Lime Sludge

Rudicler Pereira Ramos [1], Felipe Vahl Ribeiro [2], Cristian da Conceição Gomes [1], Thamires Alves da Silveira [1], Arthur Behenck Aramburu [3], Neftali Lenin Villarreal Carreno [1], Angela Azevedo de Azevedo [4] and Rafael de Avila Delucis [1,4,*]

[1] Post-Graduate Program in Materials Science and Engineering, Federal University of Pelotas, Pelotas 96010-610, Brazil; rudi.pereira@gmail.com (R.P.R.); cristianconceicao8@gmail.com (C.d.C.G.); thaamiresasilveira@gmail.com (T.A.d.S.); neftali@ufpel.edu.br (N.L.V.C.)
[2] Wood Industry Engineering, Federal University of Pelotas, Pelotas 96010-610, Brazil; felipe.vs.ribeiro@gmail.com
[3] Post-Graduate Program in Mining, Metallurgical and Materials Engineering, Federal University of Rio Grande do Sul, Porto Alegre 90650-001, Brazil; arthuraramburu@gmail.com
[4] Civil Engineering, Federal University of Pelotas, Pelotas 96010-610, Brazil; azevedoufpel@gmail.com
* Correspondence: rafael.delucis@ufpel.edu.br

Abstract

The combined effects of accelerated carbonation and lime sludge incorporation on the mechanical and durability performance of fiber-cement composites were assessed in this study. Lime sludge was used to replace 0%, 10%, and 20% of the cement in the composites, which were then autoclave-cured and carbonated more quickly for two or eight hours. With LS20-C8 (20% lime sludge, 8 h carbonation) achieving the highest carbonation efficiency (74.0%), X-ray diffraction (XRD) verified the gradual conversion of portlandite into well-crystallized calcium carbonate ($CaCO_3$). In terms of mechanical performance, LS20-C8 outperformed the control by increasing toughness by 16.7%, flexural strength by 14.2%, compressive strength by 14.6%, and compressive modulus by 20.3%. The properties of LS20-C8 were better preserved after aging under wetting-drying cycles, as evidenced by lower losses of toughness (10.0%) and compressive strength (10.1%) compared to the control (14.6% and 18.3%, respectively). The mechanical improvements were explained by optical microscopy, which showed decreased porosity and an enhanced fiber–matrix interface. Overall, the findings show that adding lime sludge to accelerated carbonation improves durability, toughness, strength, and stiffness while decreasing porosity. This method helps to value industrial byproducts and is a sustainable and efficient way to create long-lasting fiber-cement composites.

Keywords: mechanical properties; durability; fiber–matrix interface; optical microscopy; sustainable construction materials

Received: 11 July 2025
Revised: 10 September 2025
Accepted: 26 September 2025
Published: 30 September 2025

Citation: Ramos, R.P.; Ribeiro, F.V.; Gomes, C.d.C.; da Silveira, T.A.; Aramburu, A.B.; Carreno, N.L.V.; de Azevedo, A.A.; Delucis, R.d.A. Accelerated Carbonation for Improving Mechanical Performance of Sustainable Fiber-Cements Containing Lime Sludge. *Appl. Mech.* **2025**, *6*, 73. https://doi.org/10.3390/applmech6040073

1. Introduction

Fiber-cement composites have been widely used globally due to their versatility in manufacturing building elements such as flat and corrugated sheets, and pipes for walls and other surfaces. These are prevalent in most residential, agricultural, and industrial buildings, particularly in developing regions [1]. Consequently, fiber-cement is considered one of the best solutions for housing aimed at lower-income populations, owing to its reduced cost compared to other conventional construction solutions, especially for roofing [2].

Fiber-cement composites are cementitious materials consisting of a cement matrix reinforced by fibers, along with additives and supplementary materials that may be incorporated. Thus, compared to other cementitious composites like mortars and concretes, fiber-cements are distinguished by the absence of fine aggregates (such as natural or artificial sand) or coarse aggregates (like crushed stone or gravel) in their composition.

The primary objective of incorporating fibers is to mitigate the brittleness of cement, thereby improving ductility. This also ensures the maintenance of strength even after matrix cracking, allowing for greater composite deformation before rupture, and providing enhanced impact resistance and toughness [3–5]. Historically, the cement matrix was reinforced with asbestos fibers, but these have since been replaced by other synthetic or natural (vegetable) fibers, often maintaining or even improving the physical and mechanical properties of the composites [6].

Vegetable fibers offer several advantages: they are biodegradable, renewable, widely available, non-hazardous to workers, and low-cost and require less energy for manufacturing [7,8]. However, the mechanical support effect of vegetable fibers in fiber-cements can be compromised when the highly alkaline pH (above 12) of the cement curing process causes alkaline hydrolysis of these fibers [9]. To prevent this chemical attack by the matrix on the fibers, the two most common approaches in the literature are to thermally [10] or chemically [11,12] treat the fibers and to add pozzolans to the matrix to reduce its pH [13,14]. Inducing a carbonation process in the matrix represents a third option, which has been considerably less explored to date.

Carbonation involves a chemical reaction that leads to the formation of calcium carbonate ($CaCO_3$), also known as limestone. Generally, this compound is formed by the reaction of carbon dioxide (CO_2) with calcium oxide (CaO), also known as lime. According to Tonoli et al. [15], in composites reinforced with vegetable fibers, the carbonation of the composite is enhanced due to its high porosity, which facilitates CO_2 penetration, allowing $CaCO_3$ formation within the material. The consumption of alkalis (such as calcium hydroxide [$Ca(OH)_2$]), present in the material's pores, leads to a decrease in the alkalinity of the environment (pH reduction), consequently providing a less aggressive environment for the fibers. Carbonation also results in increased material densification, raising the specific mass and, consequently, the values of mechanical strength and elastic modulus.

To enhance the carbonation process and further improve mechanical performance and durability, the incorporation of calcium-rich substances has already been addressed in the literature in order to stabilize the alkaline environment and improve the matrix–fiber interaction. If supplementary materials are applied, it may contribute to sustainability through waste valorization. The integration of such residues offers a pathway towards developing more sustainable and cost-effective construction materials by simultaneously addressing waste management and enhancing material properties.

Lime sludge cellulose refers to cellulosic fibers or waste derived from paper industry sludge, often characterized by its high lime content, and has significant applications, particularly in building materials. Recent studies highlight its utility in eco-friendly construction, where incorporating cellulose fibers from waste paper sludge into cement-based mortars and bricks can yield mechanical properties (such as compression and flexural strength) comparable to conventional counterparts [16,17]. Environmentally, using lime sludge cellulose in these materials contributes to substantial waste reduction, diverting industrial byproducts from landfills, lowering disposal costs, and decreasing the demand for virgin raw materials, thereby mitigating pollution. However, challenges exist, such as water repellency issues when lime sludge is used as a filler in paper, though these can be addressed with cationic polymers [18]. Furthermore, the reactivity of fly ashes derived from

cellulose industries, which contain lime sludge, may be limited due to surface coatings and high sulfate/alkali content, impacting their efficacy in certain applications like autoclaved aerated concrete [17].

Considering the diverse advantages and limitations associated with the use of lime sludge in construction materials, the full potential of recycling this industrial byproduct for such purposes remains underexplored and its impact is not entirely clear. Therefore, this article investigates the effectiveness of accelerated carbonation as a strategy to enhance the performance of cellulose fiber-cement composites, specifically exploring the partial replacement of Portland cement with lime sludge. Figure 1 illustrates a schematic flowchart summarizing the key chemical and physical processes involved in this approach, including the hydration reactions of Portland cement, the role of lime sludge as a calcium-rich additive, the diffusion of atmospheric or injected CO_2, and the subsequent formation of calcium carbonate ($CaCO_3$) through induced carbonation.

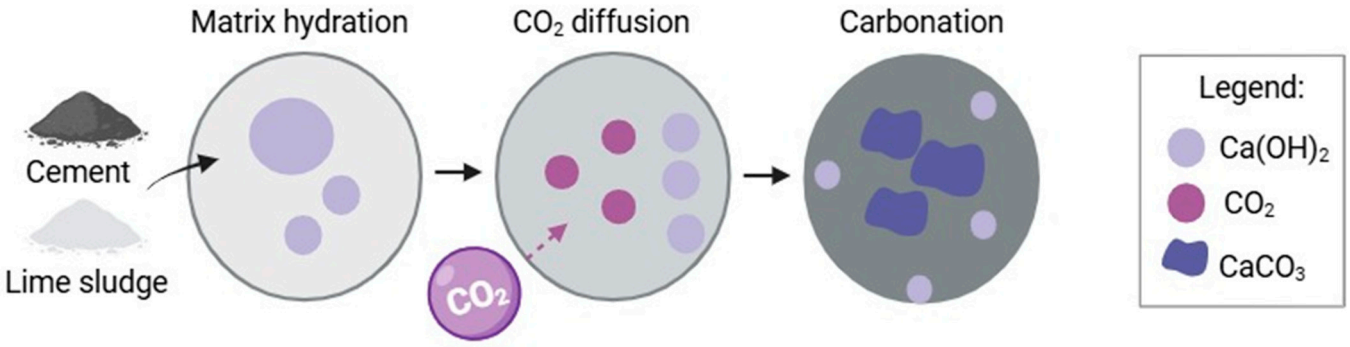

Figure 1. Schematic representation of the chemical processes involved in the production of fiber-cement composites containing lime sludge, highlighting cement hydration, CO_2 diffusion, and induced carbonation leading to $CaCO_3$ formation.

This study aimed to determine whether combining lime sludge as a partial cement replacement with accelerated carbonation can enhance the strength, stiffness, toughness, and durability of cellulose fiber-cement composites, while elucidating the underlying mineralogical/microstructural mechanisms.

2. Materials and Methods

2.1. Raw Materials

The cement utilized in this study was Votoran Obras Especiais CPV ARI RS. Its properties conformed to Brazilian standards, presenting a Blaine fineness of $\geq$3000 cm^2/g NBR NM 76 [19], an initial setting time exceeding 1 h NBR NM 65 [20], a loss on ignition below 4.5% NBR 5743 [21], an MgO content less than 6.5% NBR 9203 [22], and an SO_3 content not exceeding 4.5% NBR 5745 [23]. The particle size distribution of the Portland cement was determined using a laser diffraction granulometer (CILAS 1064 equipment—CILAS—Aubagne, France), with an analysis range spanning from 0.04 µm to 500.00 µm. The test was performed in a liquid medium with detergent as a dispersing agent, and ultrasound was applied for 60 s to ensure proper particle dispersion. The Fraunhofer approximation was employed for size calculation. The results indicate a finely distributed particle profile, consistent with high-performance cement characteristics. The cumulative volume curve shows a significant concentration of particles below 10 µm.

The cellulose fiber used was an unbleached eucalyptus kraft pulp, generously supplied by CMPC Celulose Riograndense Company (Guaíba, Brazil). According to the manufacturer's specifications, this unbleached pulp contains a residual lignin content ranging from

1.5% to 3% by weight. The studied cellulosic pulp presented a weighted average fiber length of 0.8–0.9 mm and a fiber width ranging from 19.5 to 20.6 µm.

Lime sludge was also provided by the CMPC company. This industrial byproduct originates from the causticizing stage of pulp production, where lime facilitates lignin precipitation. Post-precipitation, the lime mud is separated from the purified pulp and other impurities via a washer filter, settling or being captured to allow subsequent processing of the pulp. The company currently generates approximately 4500 tons of this residue monthly, which is primarily repurposed as a soil acidity corrector (macro-calcium). According to the supplier, this residue is mainly composed of CaO (slightly above 50%) and shows a high loss on ignition of approximately 40%. Its morphological features may be marked by irregular particles of different sizes, often forming agglomerates, likely due to the precipitation process through which the residue is generated. The X-ray diffractogram (XRD) shown in Figure 2 reveals prominent peaks at approximately 2θ = 23°, 29° (very intense), 36°, 39°, 42°, 47°, and 49°. These peaks are characteristic of crystalline phases rich in calcium compounds, confirming the presence of well-defined mineral structures within the lime sludge.

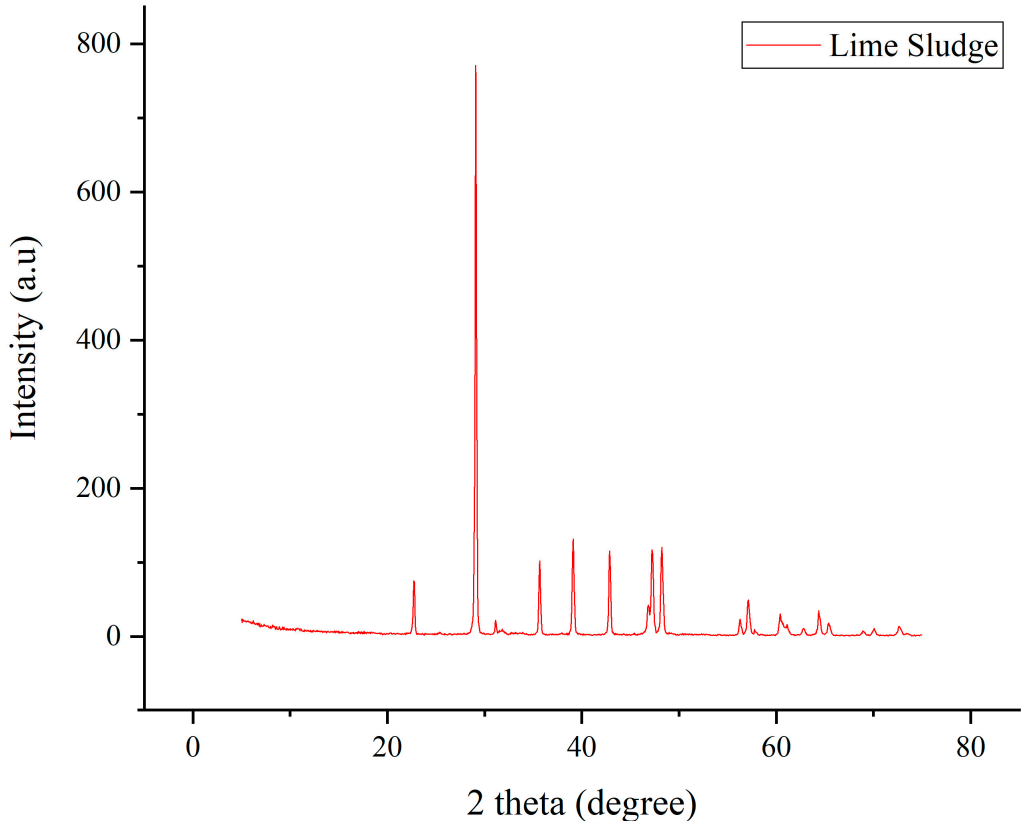

Figure 2. X-ray diffraction (XRD) pattern of the lime sludge.

For this study, the lime sludge powder was dried at 60 °C for 4 days. Subsequently, it was processed in a cylindrical tumbler ball mill containing 10 zirconia balls. The milled material was then sieved using a sieve shaker. The particle size distribution of the lime sludge was also evaluated using the already mentioned granulometer. The results revealed that the lime sludge exhibited a broader size distribution compared to the cement, with a notable proportion of particles in the range of 10–100 µm. Despite its coarser profile, the lime sludge still contains a considerable (68%) fraction of fine particles (<10 µm). Representative photographs of some raw materials are shown in Figure 3 for visual reference.

Figure 3. Some raw materials used in this study.

2.2. Composite Preparation

The composites were produced, according to Figure 4, in batches of approximately 2 kg of cementitious material. Cellulose fibers were added at 2.85% relative to the cement mass, with a water-to-cement ratio (w/c) of 0.42, in accordance with the procedure described by Silveira et al. [12]. In the formulations labeled LS10 and LS20, 10% and 20% of the cement mass were replaced by lime sludge, respectively, while the Control mixture contained only cement without any lime sludge substitution.

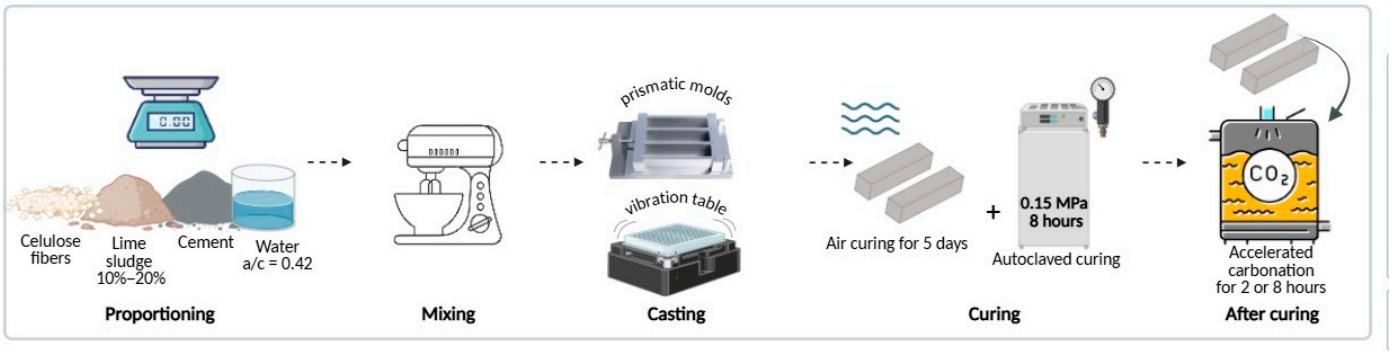

Figure 4. Schematic representation of the composite preparation and curing process, including accelerated carbonation.

Initially, the cellulose fibers were soaked in water for about 5 min to ensure complete saturation. In parallel, the cement and lime sludge (when present) were manually mixed to achieve uniform distribution. The hydrated fibers were then combined with the dry mix using a planetary mortar mixer (vertical axis), operating at 140 rpm for 3 min. This was followed by an additional mixing stage at 220 rpm for 2 min to ensure homogeneity of the paste.

As recommended by ASTM C305 [24], the fresh composite paste was cast into prismatic molds (40 mm × 40 mm × 160 mm) in two layers, with each layer compacted on a vibrating table to eliminate air voids. The specimens were left under air curing for 5 days before being demolded. After demolding, the samples were subjected to autoclave curing under a pressure of 0.15 MPa for 8 h.

The accelerated carbonation of the fiber-cement composites in this study followed a multi-stage process designed to enhance material performance. Initially, the composites underwent molding and initial curing for 24–48 h in a humid chamber, or covered with plastic sheets, to promote early hydration and strength development while preventing premature drying. This was followed by thermal curing for 8 to 24 h in an oven maintained at 60–80 °C to accelerate hydration and promote the rapid formation of calcium silicate hydrate (C-S-H) and calcium hydroxide ($Ca(OH)_2$), both essential substrates for carbonation. Subsequently, the composites were subjected to conventional humid curing for 5–7 days to allow hydration reactions to progress and ensure sufficient formation of portlandite. A controlled drying stage was then applied for 24–48 h to reduce the moisture content to below 70%, achieving a relative humidity between 50% and 70% to optimize conditions for carbonation. The accelerated carbonation was performed over a period of 2–8 h, during which the specimens were exposed to a CO_2-rich environment −(~20% CO_2) at ~20 °C with controlled humidity to promote the formation of calcium carbonate ($CaCO_3$), enhancing mechanical performance, following adaptations of the method proposed by Tonoli et al. [15]. Finally, the composites underwent a supplementary curing stage of 7 days to support continued hydration, pozzolanic activity, and potential rehydration of partially carbonated phases.

To concisely identify experimental groups, a naming convention is used: “LS” (lime sludge) followed by the percentage of cement replacement (10 or 20), then “C” (carbonation) and the treatment duration in hours (2 or 8). For example, “LS10-C2” signifies 10% lime sludge replacement with 2 h of carbonation. The “Control” group serves as the baseline, without lime sludge or induced carbonation. Natural aging of the cementitious composites was simulated through a series of wetting and drying cycles. Each cycle was set for a duration of 48 h. This involved drying the samples in an oven at 65 °C for 24 h, followed by immersion in water for another 24 h. A total of 40 such wetting and drying cycles were performed, accumulating to a simulated aging period of 80 days.

2.3. Characterization Techniques

X-ray Diffraction (XRD) patterns were recorded using a Bruker D8 Advance diffractometer (Bruker, MA, USA). The instrument operated with copper Kα radiation (λ = 0.15406 nm) and scanned in the 2θ range of 10–80°, with a step size of 0.05°/s and 12 mm slits. The XRD data were processed to quantify the phase transformations induced by carbonation and the incorporation of lime sludge in the composites. The analysis focused on identifying and integrating the characteristic peaks of portlandite ($Ca(OH)_2$) and calcite ($CaCO_3$), the key phases involved in the carbonation process. The main diffraction peak for portlandite was considered at approximately 2θ = 18.0° (001 reflection), which is the most intense and distinctive signal for this phase, while the main peak for calcite was identified at approximately 2θ = 29.4° (104 reflection), which represents its strongest and most reliable signature. The areas under these peaks were integrated after baseline correction to quantify their relative abundance. From these integrated areas, the ratio of calcite to portlandite was calculated to evaluate the extent of the carbonation reaction and the mineralogical transformation that occurred in the composite matrix. Additionally, the

relative content of calcite with respect to the sum of both phases was determined, providing a direct measure of carbonation efficiency (% $CaCO_3$).

$$\% \, CaCO_3 = \frac{Area_{CaCO3} + Area_{Ca(OH)2}}{Area_{CaCO3}} \times 100 \quad (1)$$

The mechanical behavior of the composites was assessed through three-point bending and uniaxial compression tests, following the procedures outlined in ASTM C348 [25]. Flexural tests were conducted using a universal testing machine (EMIC DL 30000—Instron Brasil—São Jose dos Pinhais, Paraná, Brazil) with a span of 100 mm and a loading rate of 50 N/s until failure. Based on data for both force (F) and the vertical displacement (δ) at the specimen's upper face, flexural stress (σ_x), strain (ϵ_x), and flexural toughness were calculated. The flexural stress at a given load, the corresponding flexural strain (relating specimen height, span length, and measured displacement), and the flexural strength (σ_f), defined as the maximum stress sustained before failure, were all determined. The flexural toughness was subsequently computed as the area under the stress–strain curve using OriginPro 8.5 (SR1) software. All these properties were calculated according to the methodology described by Silveira et al. [12]. Following the flexural test, one side of each fractured specimen was subjected to a uniaxial compression test, also in accordance with ASTM C348 [25]. This test was performed using the same universal testing machine, employing prismatic platens (40 mm × 40 mm) and a loading rate of 500 N/s. During the test, load and displacement were recorded and subsequently converted into stress and strain, using Equations (1) and (2). The compressive strength (σ_c) was determined, and the compressive modulus of elasticity (E_c) was calculated as the slope of the linear portion of the stress–strain curve, defined between 0.5 MPa and 30% of σ_c. These properties were also calculated according to the methodology described by Silveira et al. [12].

$$\sigma_c = F/A \quad (2)$$

$$\varepsilon_c = \Delta L/L_0 \quad (3)$$

where σ_c = compressive stress (MPa); F = applied force (N); A = cross-sectional area of the specimen (mm^2); ε_c = compressive strain (mm/mm); ΔL = recorded axial displacement (mm); L_0 = initial height of the specimen (mm).

The bulk density of the specimens was calculated from their oven-dried mass and corresponding geometric volume. To evaluate apparent porosity and water absorption, the samples were immersed in water for 24 h. After this period, three mass conditions were recorded: submerged, saturated surface-dry, and oven-dry. These measurements were then used to estimate the open pore volume and the water uptake of the composites. The procedure followed the guidelines of ASTM C948 [26], which establishes the relationships among these values to determine the accessible void fraction and the water-holding capacity, as also described by Gutiérrez et al. [4].

Optical microscopy was employed to examine the microstructural features of the fiber-cement composites, with a particular focus on pore distribution, matrix densification, and the fiber–matrix interface. Samples were first sectioned into smaller pieces using a low-speed diamond saw to minimize the introduction of microcracks. The resulting cross-sections were then dried in a desiccator at room temperature to remove any residual moisture, preventing artifacts during the polishing process. Surface preparation involved sequential polishing with silicon carbide abrasive papers, followed by a final polish with a 1 µm diamond suspension to achieve a smooth and reflective surface. To enhance contrast between the matrix and voids, selected polished sections were treated with a phenolphthalein indicator solution. Prior to application, surfaces were lightly dried with

absorbent paper to remove excess moisture that could dilute the indicator. The phenolphthalein solution (0.5% in ethanol or hydroalcoholic medium) was applied uniformly using a soft brush to avoid pooling or streaking. The coloration response was monitored within 5 to 30 s, as the pink hue indicating uncarbonated regions develops rapidly. After this brief period, the surface was allowed to air-dry just enough for excess solution to evaporate (1–2 min), ensuring that the color remained vivid for imaging. Samples were observed under a reflected light microscope, equipped with a digital camera. Images were captured from multiple regions of interest to ensure representativeness of the microstructural characteristics.

3. Results and Discussion

The XRD patterns (Figure 5) visually illustrate significant mineralogical transformations induced by the carbonation process and the presence of lime sludge. No anomalous or unexpected phases were detected, confirming the controlled nature of the chemical reactions and the validity of the results within the context of cementitious materials. For the control samples (0% lime sludge and uncarbonated), prominent peaks corresponding to portlandite (calcium hydroxide, $Ca(OH)_2$) were observed, especially at $2\theta = 18.0^\circ$, along with peaks for unreacted cement phases. As carbonation time increases and lime sludge content is introduced, a clear reduction in the intensity of portlandite peaks was observed. Concomitantly, new and increasingly intense peaks corresponding to calcium carbonate ($CaCO_3$), specifically calcite at $2\theta = 29.4^\circ$, emerge and strengthen. This trend is particularly evident in the LS20-C8 group (20% lime sludge, 8 h carbonation), where the portlandite peaks are significantly diminished, and the calcite peaks show the highest intensity and sharpness, indicating a high degree of crystallization. This qualitative observation is supported by the quantitative data presented in Table 1, which shows a progressive increase in the integrated area of calcite peaks and a corresponding rise in % $CaCO_3$ from 66.8% in the control to 74.0% in LS20-C8. These values provide numerical confirmation of the enhanced carbonation efficiency associated with greater lime sludge content and extended carbonation duration. This reaction densifies the matrix and reduces alkalinity, which preserves cellulose fibers and strengthens the fiber–matrix interface.

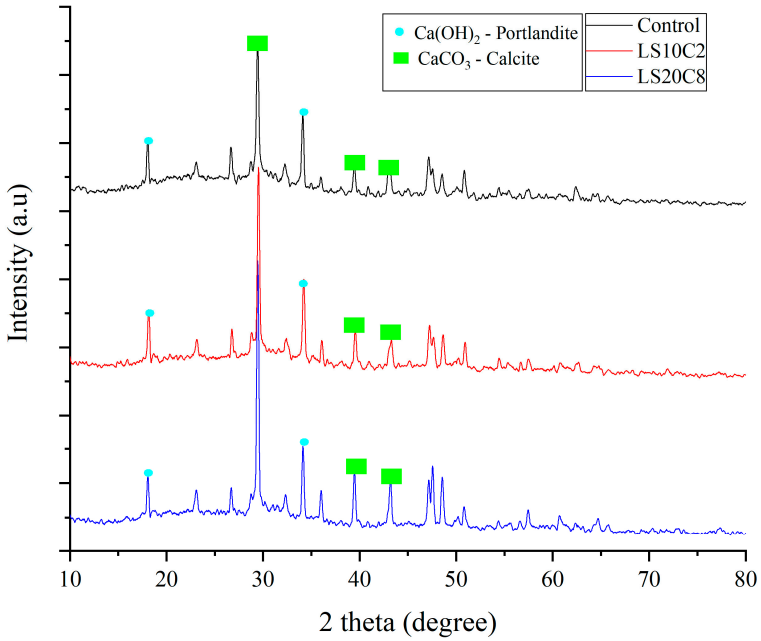

Figure 5. XRD patterns of fiber-cement composites with 0%, 10%, and 20% lime sludge after 2 and 8 h of accelerated carbonation.

Table 1. Quantitative analysis of XRD peak areas for portlandite and calcite, and corresponding carbonation efficiency (% $CaCO_3$).

Sample	$Ca(OH)_2$ Area	$CaCO_3$ Area	% $CaCO_3$
Control	61.73	124.02	66.8%
LS10-C2	56.57	134.75	70.4%
LS20-C8	55.02	156.78	74.0%

Theoretically, carbonation involves the reaction of atmospheric carbon dioxide (CO_2) with calcium hydroxide present in the cement matrix to form calcium carbonate and water. This reaction is represented as: $Ca(OH)_2 + CO_2 \rightarrow CaCO_3 + H_2O$. The accelerated carbonation process intensifies this reaction. The presence of lime sludge, a calcium-rich byproduct, provides an additional source of calcium ions, effectively boosting the formation of calcium carbonate. This not only consumes the alkaline $Ca(OH)_2$, which lowers the matrix's pH and creates a less aggressive environment for the cellulose fibers (thereby reducing fiber degradation), but also fills pore spaces, leading to increased material density and reduced porosity. The higher crystallinity of calcite observed in samples with increased lime sludge and carbonation time suggests a more complete and efficient carbonation reaction, resulting in a more stable and stronger microstructure. These XRD findings are highly consistent with established literature on carbonation of cementitious materials. Studies, like León-Martínez et al. [27], consistently report the transformation of portlandite into calcite and aragonite (another $CaCO_3$ polymorph) upon carbonation, which leads to pore refinement and enhanced mechanical properties. The observation that increased calcium availability promotes more extensive carbonation aligns with the principles of chemical equilibrium and reactant availability in such systems.

In Figure 6a, it is observed that, for the unaged composites, the compressive strength shows a general increase with the incorporation of lime sludge and carbonation treatment. Comparatively to the control group with 32.8 MPa, the LS20-C8 group stood out, reaching 37.6 MPa, representing an increase of approximately 14.6%. Even the groups with 10% lime sludge (LS10-C2 and LS10-C8) showed improvements, with increments of about 1.22% and 8.23%, respectively. After aging, all groups exhibited a reduction in compressive strength compared to their unaged counterparts. The aged control group exhibited a 14.63% decrease compared to its unaged state. However, the aged LS20-C8 formulation maintained the highest strength, 33.8 MPa, with a smaller percentage loss of approximately 10.1% compared to its unaged condition, suggesting greater durability.

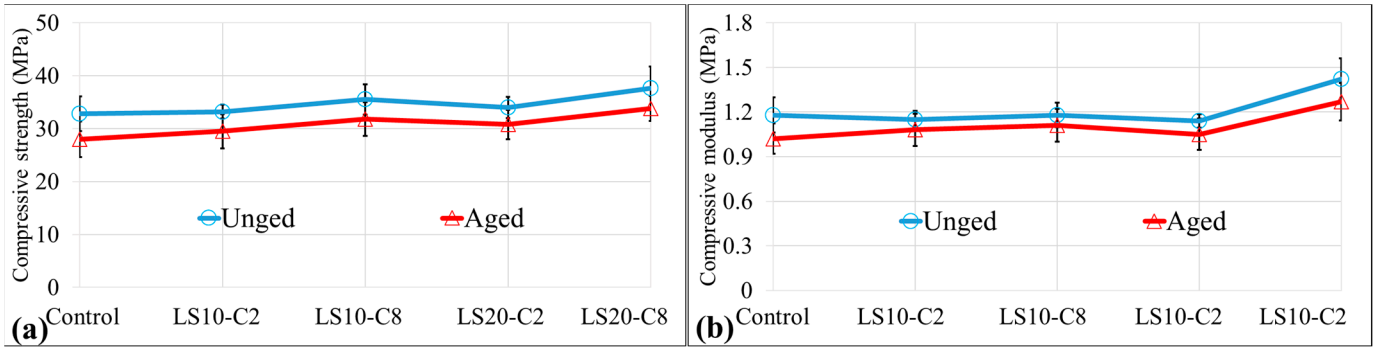

Figure 6. Compressive strength (**a**) and modulus (**b**) of fiber-cement composites with and without aging.

In Figure 6b, the compressive modulus values followed a similar trend to strength. In the unaged composites, the modulus of the control group was 1.18 MPa. The LS20-C8

group again demonstrated the best performance, with a modulus of 1.42 MPa, representing a gain of approximately 20.34% relative to the control. Similarly, the LS10-C2 and LS10-C8 groups showed increases of approximately 5.88% and 8.82%, respectively. After aging, the compressive modulus also decreased in all groups. The aged Control group had a reduction of 13.56% (1.02 MPa) relative to the unaged condition. The percentage loss in modulus was smaller (c.a. 10.56%) for the carbonated lime sludge groups, especially the aged LS20-C8, which recorded 1.27 MPa, indicating greater material stability under wetting and drying cycles.

These results can be explained by the densification of the cementitious matrix due to the formation of calcium carbonate ($CaCO_3$) during carbonation, as discussed in Section 1 and optical microscopy results. As confirmed by XRD patterns presented in Figure 5, the carbonation process effectively converted portlandite into well-crystallized calcium carbonate, especially noticeable in samples with 20% lime sludge and longer carbonation times (LS20-C8). The presence of calcium-rich lime sludge provides additional substrate for this reaction, enhancing the effect. Carbonation consumes calcium hydroxide [$Ca(OH)_2$], reducing the alkalinity of the medium and promoting a more favorable environment for the preservation of cellulose fibers, which contributes to maintaining the integrity of the fiber-matrix interface and, consequently, to mechanical performance. The improvement in strength and modulus, especially for longer carbonation times and higher lime sludge contents, is consistent with literature describing carbonation as a process that refines pore structure and increases material density. The lower loss of strength and modulus in the aged lime sludge and carbonated groups, compared to the Control, indicates that these treatments enhance the material's durability against degradation from wetting and drying cycles.

Results from other studies also corroborate these observations. Research by Dos Santos et al. [28] and Ballesteros et al. [29] highlights that the carbonation of vegetable fiber-reinforced cementitious composites can lead to greater densification and improved mechanical properties due to $CaCO_3$ formation and matrix pH reduction, protecting the fibers. Furthermore, the incorporation of calcium-rich residues, such as lime sludge, is a recognized strategy to increase sustainability and optimize carbonation reactions in construction materials, aligning with current trends in industrial waste valorization. The consistency of these findings with existing literature confirms the validity of the results obtained in this work and the effectiveness of the strategies employed.

The representative stress–strain curves shown in Figure 7 displayed an initial linear elastic region, followed by a peak stress point, and then a gradual post-peak softening behavior leading to eventual failure. Visually, the curves for carbonated composites, particularly those with lime sludge incorporation, exhibit higher peak stresses and steeper initial slopes compared to the control group, reflecting their superior strength and stiffness. Similarly, the initial slope of the LS20-C8 curve in Figure 7 appears notably steeper than that of the control, corresponding to the increase in compressive modulus reported in Figure 6b.

Furthermore, certain carbonated groups show a broader post-peak region, indicating enhanced deformability and energy absorption capacity. These observed enhancements in both peak stress and initial stiffness can be directly linked to the microstructural improvements. The carbonation process, intensified by the calcium-rich lime sludge, leads to significant densification of the cementitious matrix through the formation of calcium carbonate ($CaCO_3$). This pore refinement and increased matrix density contribute to the material's enhanced load-bearing capacity and rigidity. Moreover, the consumption of calcium hydroxide [$Ca(OH)_2$] during carbonation reduces the matrix's alkalinity, creating a less aggressive environment for the cellulose fibers. This protection minimizes fiber degradation and preserves the integrity of the fiber-matrix interface, allowing for more

effective stress transfer and a more ductile post-peak response, as indicated by broader softening regions in the stress–strain curves. The shape and characteristics of these stress–strain curves are consistent with observations from previous studies on fiber-reinforced cementitious composites. For example, research by Wei and Meyer [30] described similar ductile post-peak behavior in fiber-cement systems, where fiber bridging mechanisms contribute to maintaining integrity beyond the peak load. The consistent behavior of the curves across different formulations, with clear differentiation based on treatment, confirms the reliability of the experimental methodology and the robust impact of carbonation and lime sludge incorporation on the mechanical performance of these composites.

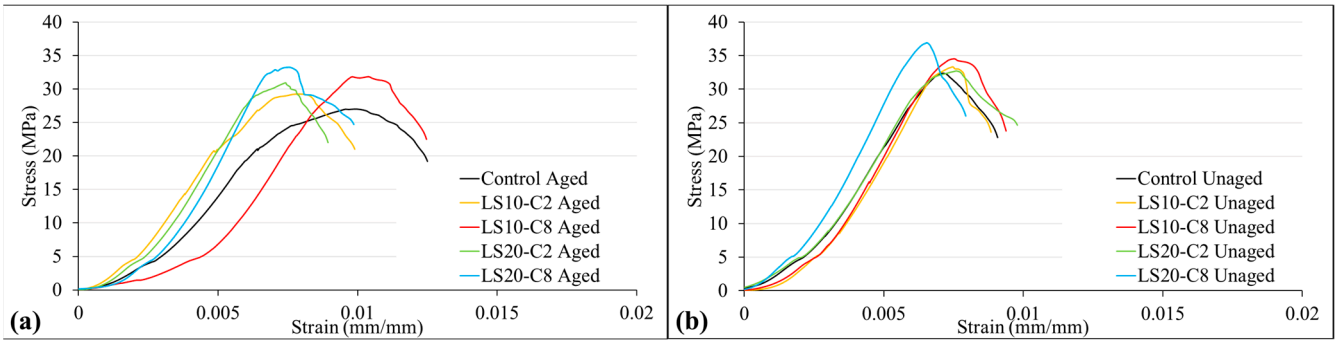

Figure 7. Representative stress–strain curves from compressive testing of aged (**a**) and unaged (**b**) fiber-cement composites.

Figure 8 illustrates the flexural strength and maximum deflection (strain at break) of fiber-cement composites, both in unaged and aged conditions. In the unaged state, the flexural strength generally increased with the incorporation of lime sludge and carbonation. The Control group exhibited a flexural strength of 4.50 MPa. Notably, the LS20-C8 group (20% lime sludge, 8 h carbonation) achieved the highest flexural strength at 5.14 MPa, representing an approximate 14.22% increase compared to the control. The LS10-C8 group also showed a significant improvement of about 7.52%. For maximum deflection, the control group showed 0.45 mm. The LS20-C8 group reached 0.48 mm, indicating a 6.67% increase in deformability, suggesting enhanced ductility.

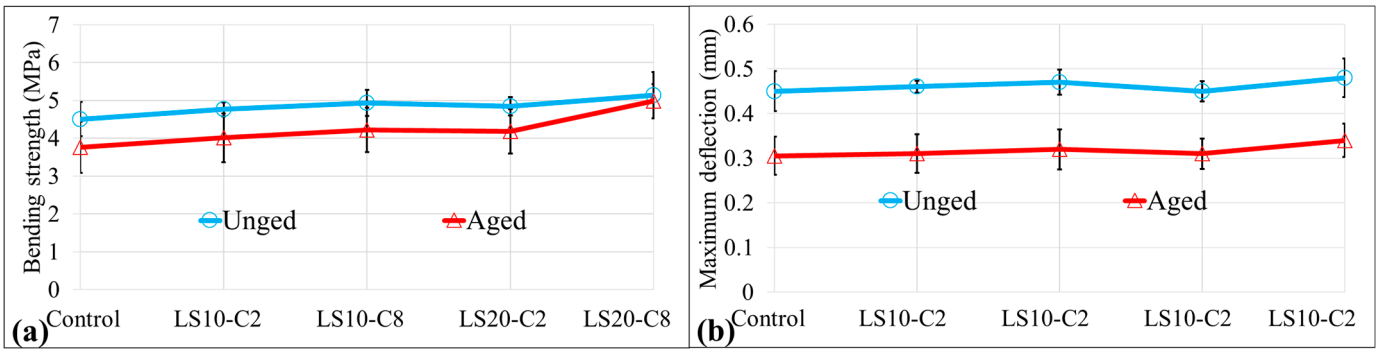

Figure 8. Bending strength (**a**) and strain at break (**b**) of fiber-cement composites with and without aging.

Upon aging, all composites experienced reduction in both flexural strength and maximum deflection. The aged control group's flexural strength dropped to 3.76 MPa, a decrease of approximately 16.55% from its unaged counterpart. Similarly, its maximum deflection was reduced to 0.305 mm, a substantial loss of about 32.22%. In contrast, the aged LS20-C8 formulation exhibited superior retention of properties. While its flexural strength was reduced to 4.98 MPa, this represented a loss of only 3.11% from its unaged state, signifi-

cantly outperforming the control's retention. Its aged maximum deflection was 0.34 mm, a 29.17% reduction from its unaged condition, which, although a decrease, positioned it as the best-performing aged group.

These improvements in flexural performance, particularly the superior retention of properties in carbonated composites with lime sludge, are directly linked to the enhanced densification of the cementitious matrix and improved fiber-matrix interaction. As evidenced by the XRD patterns in Figure 5, carbonation effectively transforms portlandite into well-crystallized calcium carbonate, especially pronounced in samples with 20% lime sludge and extended carbonation times (LS20-C8). This conversion not only densifies the matrix, contributing to increased strength (consistent with the compressive strength results in Figure 6a, but also consumes calcium hydroxide [$Ca(OH)_2$]. The reduction in matrix alkalinity provides a less aggressive environment for the cellulose fibers, mitigating alkaline degradation and preserving fiber integrity. This enhanced fiber protection is crucial for maintaining the composite's ability to deform and absorb energy, leading to higher maximum deflections and improved post-peak behavior.

The observed trends align well with existing literature on fiber-reinforced cementitious composites. Studies by Gutíerrez et al. [4] and Da Silveira et al. [12] have reported similar improvements in flexural strength and ductility in composites where fiber-matrix adhesion is enhanced or fiber degradation is mitigated, which were ascribed to fiber treatment or pozzzolan addition. The increased flexural strength in carbonated samples is consistent with the established understanding that $CaCO_3$ formation improves matrix density and strength. Furthermore, the ability of the LS20-C8 group to retain a high percentage of its initial flexural strength and deformability after aging cycles corroborates findings in the literature that highlight the role of carbonation in enhancing the long-term durability of fiber-cement systems [31,32]. No significant anomalies were observed, reinforcing the validity of the results and confirming the beneficial effects of lime sludge and accelerated carbonation on flexural toughness.

Figure 9 illustrates the flexural toughness of fiber-cement composites under both unaged and aged conditions. In the unaged state, the flexural toughness generally increased with the incorporation of lime sludge and carbonation. The Control group exhibited a toughness of 66 J/m^3. The LS20-C8 group (20% lime sludge, 8 h carbonation) achieved the highest toughness at 77 J/m^3, representing an approximate 16.67% increase compared to the Control. Other carbonated groups also showed improvements: LS10-C2 increased by approximately 4.17% (68.75 J/m^3), LS10-C8 by approximately 10.83% (73.15 J/m^3), and LS20-C2 by approximately 4.99% (69.3 J/m^3) relative to the Control. Upon aging, all composites experienced a reduction in flexural toughness. The aged Control group's toughness dropped to 53.9 J/m^3, a significant decrease of approximately 18.33% from its unaged counterpart. However, the aged LS20-C8 formulation demonstrated superior retention, with a toughness of 69.3 J/m^3, representing a loss of only 10.00% compared to its unaged state, indicating enhanced durability against environmental degradation. This superior retention in LS20-C8 significantly outperforms other aged groups, which experienced losses ranging from 12.70% (LS20-C2) to 18.33% (Control).

These improvements in flexural toughness are closely linked to the overall enhanced mechanical performance and microstructural changes observed in the composites. The densification of the cementitious matrix due to calcium carbonate ($CaCO_3$) formation during carbonation, as confirmed by XRD in Figure 5, contributes to a more robust and energy-absorbing material. This densification, in turn, is consistent with the increased compressive strength and modulus shown in Figure 6. The presence of lime sludge, a calcium-rich by-product, amplifies these carbonation effects by providing additional precursors for $CaCO_3$ formation, which also leads to a reduction in the highly alkaline

environment around the cellulose fibers. This less aggressive environment, coupled with improved fiber-matrix interaction (as suggested by the flexural strength and maximum deflection in Figure 8), allows the fibers to more effectively bridge cracks and absorb energy, thereby increasing the composite's overall toughness and its ability to resist crack propagation before catastrophic failure.

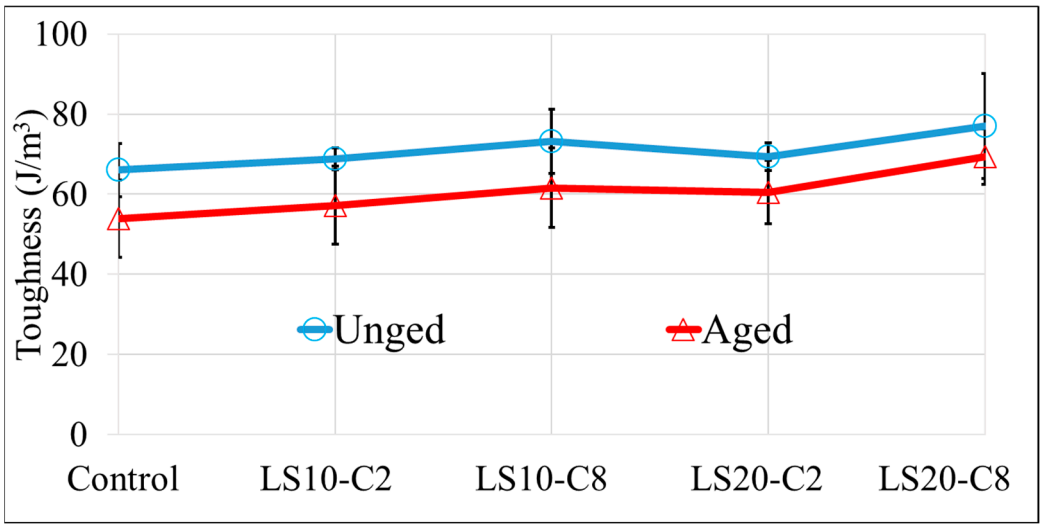

Figure 9. Toughness under flexural loading of fiber-cement composites with and without aging.

The trends observed for flexural toughness are in strong agreement with existing literature on fiber-reinforced cementitious composites. Studies by Neves Junior et al. [33] have reported that matrix modifications, such as the addition of pozzolans or pH reduction via carbonation, can significantly enhance fiber-matrix bonding and, consequently, bending properties. The improved energy absorption capacity, particularly evident in the LS20-C8 group, corroborates findings that link denser microstructures and better fiber-matrix interfaces to superior mechanical performance, including toughness. For instance, the general trend of increased toughness in carbonated samples is well-established in research focusing on the long-term performance of cement-based materials [34].

Figure 10 presents the representative stress–strain curves obtained from the three-point bending tests of the fiber-cement composites, under both unaged and aged conditions. Visually, these curves typically display an initial linear elastic region, a peak load, and a subsequent post-peak softening behavior, characteristic of fiber-reinforced cementitious materials where fibers provide residual strength after matrix cracking. For the unaged composites, the curves for groups incorporating lime sludge, particularly LS20-C8 (20% lime sludge, 8 h carbonation), exhibit higher peak loads and extended deflection ranges compared to the Control. This indicates superior flexural strength and enhanced ductility. For example, the peak load for LS20-C8 appears notably higher, reflecting its approximately 14.05% increase in flexural strength relative to the Control, as quantified in Figure 8. The longer tail in the post-peak region for LS20-C8 also visually corresponds to its higher maximum deflection (6.67% increase compared to Control, as seen in Figure 8) and superior flexural toughness (16.67% increase, as shown in Figure 9), signifying greater energy absorption capacity. Upon aging, all curves show a reduction in both peak load and maximum deflection, indicating a decrease in mechanical performance. However, aged LS20-C8 demonstrates remarkable retention of its load-bearing capacity and deformability, maintaining a higher peak load and a more extended deflection range compared to the aged Control, consistent with its superior retention of flexural strength and toughness (Figures 8 and 9).

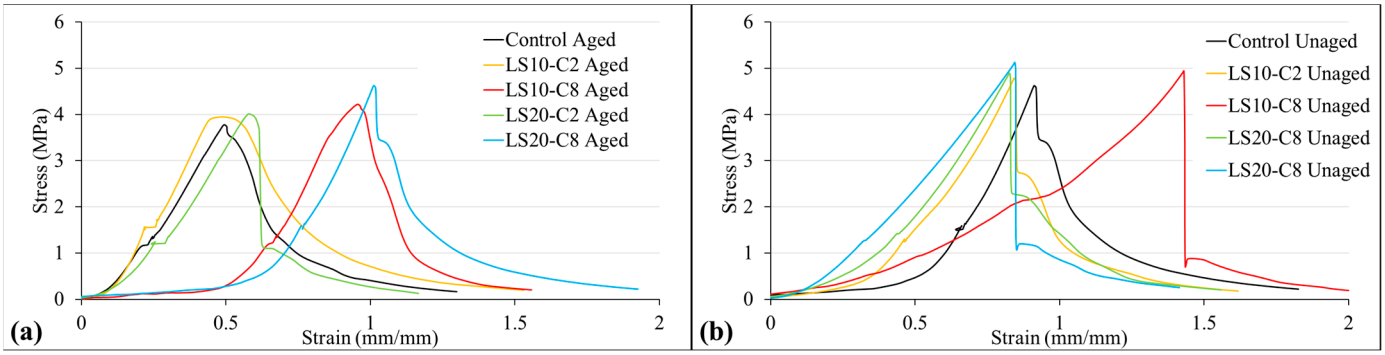

Figure 10. Representative stress–strain curves from three-point bending tests of fiber-cement composites with (**a**) and without aging (**b**). Where: LS10 and LS20 are related to samples containing 10% and 20% of lime sludge, respectively; C2 and C8 mean 2 h and 8 h of carbonation, respectively.

These stress–strain characteristics are primarily attributed to the microstructural modifications induced by carbonation and lime sludge incorporation. The formation of well-crystallized calcium carbonate ($CaCO_3$), particularly pronounced in LS20-C8 as confirmed by XRD patterns in Figure 5, leads to significant matrix densification. This improved density enhances the overall load-bearing capacity, contributing to higher peak loads. Furthermore, the consumption of calcium hydroxide [$Ca(OH)_2$] by the carbonation reaction, facilitated by the calcium-rich lime sludge, reduces the matrix's alkalinity. This creates a less aggressive environment for the cellulose fibers, protecting them from alkaline degradation and preserving the integrity of the fiber-matrix interface. An intact and strong interface allows for more efficient stress transfer from the matrix to the fibers, enabling the fibers to effectively bridge cracks, delay catastrophic failure, and contribute to the ductile post-peak behavior and increased maximum deflection observed in the curves.

The stress–strain behavior observed in this study is consistent with findings in the literature on fiber-reinforced cementitious composites. Studies by Ardanuy et al. [7] and Lima et al. [35] have widely reported similar ductile responses, where fiber bridging mechanisms are critical for controlling crack propagation and enhancing the composite's energy absorption capabilities. The improved performance in both peak load and post-peak behavior for carbonated and lime sludge-modified composites aligns with research indicating that matrix refinement and enhanced fiber protection lead to superior mechanical properties [28,36]. The consistency of these bedding features with established principles and previous works validates the effectiveness of accelerated carbonation, combined with lime sludge, in developing fiber-cement composites with improved mechanical performance and enhanced durability.

In Figure 11a, the bulk density results demonstrate that the incorporation of lime sludge and carbonation treatment consistently enhanced the compactness of the fiber-cement composites. The control group presented a density of 1.49 g/cm^3, while all modified groups achieved higher values. The LS10-C8 formulation (10% lime sludge, 8 h carbonation) reached 1.58 g/cm^3, and the LS20-C8 formulation (20% lime sludge, 8 h carbonation) exhibited the highest density at 1.60 g/cm^3, corresponding to an increase of approximately 7.0% compared to the control. These gains in density reflect the progressive densification of the matrix due to the precipitation of calcium carbonate ($CaCO_3$), which efficiently fills pore spaces and strengthens the solid structure of the composites.

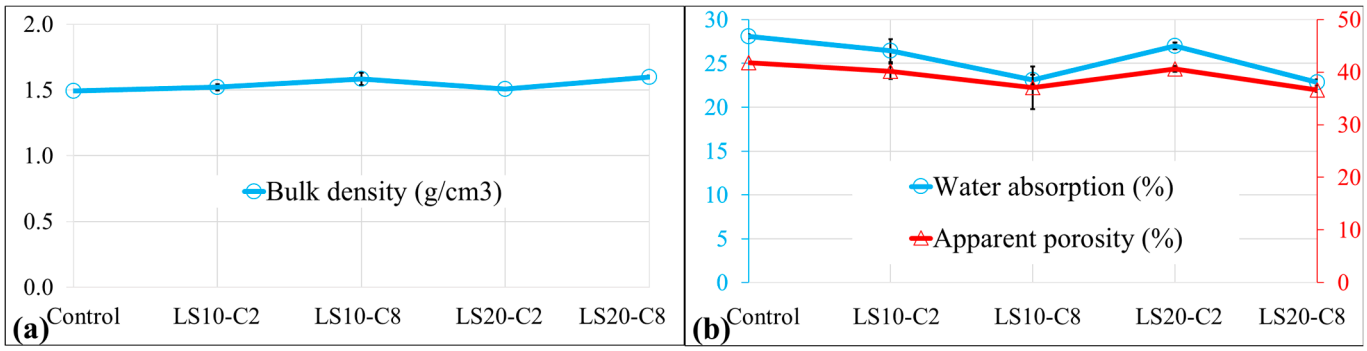

Figure 11. Bulk density (**a**), water absorption and apparent porosity (**b**) of fiber-cement composites.

In Figure 11b, the water absorption and apparent porosity values showed clear decreasing trends with increasing carbonation duration and lime sludge content. The control group had the highest water absorption (28.07%) and porosity (41.79%). With the introduction of lime sludge and carbonation, both properties declined substantially. For instance, the LS10-C8 group recorded water absorption of 23.13% and porosity of 37.03%, while the LS20-C8 formulation achieved the lowest values: 22.84% absorption and 36.64% porosity, representing reductions of 18.6% and 12.3% compared to the control, respectively. These results confirm that carbonation, intensified by the additional calcium supplied by lime sludge, not only transforms portlandite into well-crystallized calcite but also refines the pore structure, effectively limiting water ingress and decreasing the fraction of accessible voids. Comparable findings have been reported in the literature, where carbonation is identified as a mechanism that fills pores, reduces water absorption, and enhances the dimensional stability of fiber-cement composites [27–29,33].

Figure 12 presents optical microscopy images that illustrate the microstructural differences between the control and carbonated fiber-cement composite samples, with specific focus on pore distribution and the fiber–matrix interface. Figure 12a, representing the control group, shows a relatively porous matrix, with interconnected voids and noticeable gaps at the fiber–matrix interface, indicating limited bonding and a less cohesive microstructure. The application of phenolphthalein to this sample would result in an intense pink to purple coloration, confirming its highly alkaline nature and the absence of carbonation.

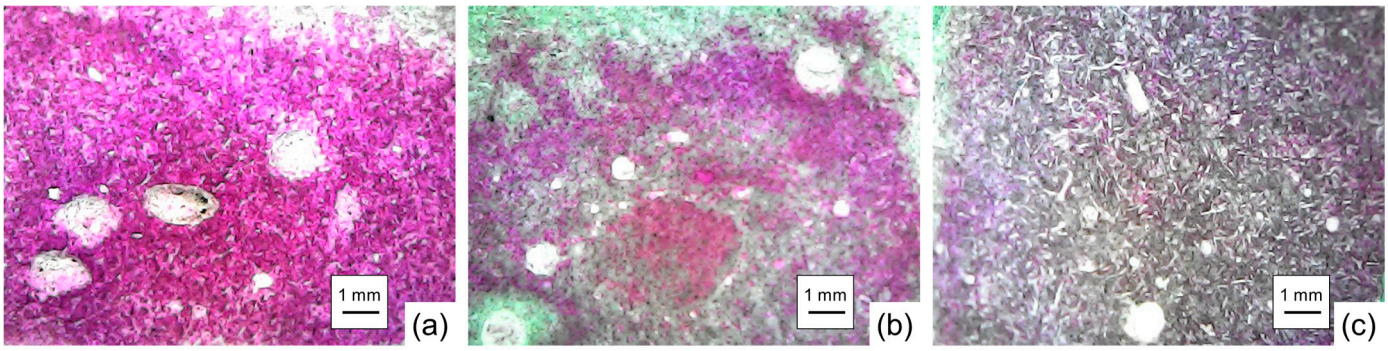

Figure 12. Optical microscopy images showing microstructural differences in pore distribution and fiber–matrix interface in (**a**) control, (**b**) LS10-C2 and (**c**) LS20-C8.

In contrast, Figure 12b, corresponding to LS10-C2, demonstrates a partially carbonated microstructure. There is a moderate reduction in porosity compared to the control. The phenolphthalein test yielded a partial decolorization, reflecting an intermediate stage of carbonation and a gradual pH reduction. Figure 12c, corresponding to LS20-C8, exhibits a much denser matrix with significantly reduced pore volume and enhanced continuity

of the cementitious phase. The fiber–matrix interface is noticeably tighter, suggesting better encapsulation of fibers. In this case, phenolphthalein would yield mostly colorless or lightly colored regions, indicating the presence of calcium carbonate and a deeper carbonation front.

These observations correlate with the improvements in mechanical properties. The densification observed in images (b) and (c), especially in sample (c), directly relates to the increased compressive and flexural strengths shown in Figures 6 and 8. Furthermore, the enhanced fiber–matrix integration supports higher deflection and toughness values, as illustrated in Figures 8 and 9, due to improved stress transfer and energy dissipation capacity. The microstructural changes are consistent with the chemical transformations identified by XRD in Figure 5, confirming the conversion of portlandite into well-crystallized calcium carbonate in carbonated samples. This process fills pores, reduces porosity, and lowers the matrix pH, providing a more favorable environment for cellulose fibers. Consequently, the degradation of fibers is minimized, preserving their reinforcing capability and structural contribution to the composite.

These results are in agreement with findings by Tonoli et al. [15] and Azevedo et al. [31], who consistently demonstrated that carbonation leads to a denser matrix and improved mechanical performance in fiber-reinforced cementitious composites. Similarly, the importance of a well-integrated fiber-matrix interface, as observed here, for increasing toughness and preventing premature failure, is widely documented [35]. The visual evidence of improved microstructural quality in the carbonated samples, particularly those with lime sludge, further validates the effectiveness of the proposed strategies and aligns with the expected behavior of such modified materials.

4. Conclusions

This study sought to investigate the impact of lime sludge incorporation and accelerated carbonation on fiber-cement composites, aiming to enhance mechanical performance, durability, and microstructural integrity while valorizing industrial by-products.

- Accelerated carbonation effectively promoted the transformation of portlandite into well-crystallized $CaCO_3$, with carbonation efficiency reaching 74.0% in LS20-C8;
- Incorporation of lime sludge, particularly at 20%, provided additional calcium sources that intensified carbonation and matrix densification;
- Mechanical performance was significantly improved in LS20-C8, with compressive strength increased by 14.6%, compressive modulus by 20.3%, flexural strength by 14.2%, and toughness by 16.7% compared to the control;
- Durability under aging (wetting–drying cycles) was enhanced, as LS20-C8 exhibited lower losses in compressive strength (10.1%) and toughness (10.0%) relative to the control;
- Bulk density, water absorption, and apparent porosity results (Figure 10) further confirmed matrix densification and pore refinement in carbonated composites, with LS20-C8 presenting the highest density and lowest porosity and absorption, which directly support the enhanced durability and reduced permeability of the material;
- Optical microscopy revealed reduced porosity and improved fiber–matrix interface in carbonated composites, explaining the superior mechanical behavior;
- The combined use of lime sludge and accelerated carbonation represents a sustainable and effective approach for producing high-performance, durable fiber-cement composites, while contributing to the valorization of industrial residues.

Author Contributions: Conceptualization, R.P.R., R.d.A.D. and T.A.d.S.; methodology, R.P.R., F.V.R. and T.A.d.S.; software, F.V.R.; validation, R.P.R., F.V.R. and C.d.C.G.; formal analysis, C.d.C.G., A.B.A.

and T.A.d.S.; investigation, R.P.R., F.V.R., C.d.C.G. and T.A.d.S.; resources, N.L.V.C. and A.A.d.A.; data curation, F.V.R., C.d.C.G. and T.A.d.S.; writing—original draft preparation, R.P.R., F.V.R. and T.A.d.S.; writing—review and editing, R.d.A.D., N.L.V.C. and T.A.d.S.; visualization, A.B.A., N.L.V.C. and T.A.d.S.; supervision, R.d.A.D.; project administration, R.d.A.D.; funding acquisition, R.d.A.D. All authors have read and agreed to the published version of the manuscript.

Funding: This work was supported by Rio Grande do Sul State Research Foundation (FAPERGS), Coordination for the Improvement of Higher Education–CAPES (code 001) and National Council for Scientific and Technological Development–CNPq (code: 304108/2024-3).

Institutional Review Board Statement: Not Applicable.

Informed Consent Statement: Not Applicable.

Data Availability Statement: The original contributions presented in this study are included in the article. Further inquiries can be directed to the corresponding author.

Conflicts of Interest: The authors declare no conflicts of interest.

References

1. Sadrolodabaee, P.; Claramunt, J.; Ardanuy, M.; de la Fuente, A. Mechanical and Durability Characterization of a New Textile Waste Micro-Fiber Reinforced Cement Composite for Building Applications. *Case Stud. Constr. Mater.* **2021**, *14*, e00492. [CrossRef]
2. Filho, M.V.A.P.M.; da Costa, B.B.F.; Najjar, M.; Figueiredo, K.V.; de Mendonça, M.B.; Haddad, A.N. Sustainability Assessment of a Low-Income Building: A BIM-LCSA-FAHP-Based Analysis. *Buildings* **2022**, *12*, 181. [CrossRef]
3. Khan, M.; Cao, M.; Ali, M. Cracking Behaviour and Constitutive Modelling of Hybrid Fibre Reinforced Concrete. *J. Build. Eng.* **2020**, *30*, 101272. [CrossRef]
4. Gutiérrez, M.A.U.; da Silveira, T.A.; Ribeiro, F.V.; Aramburu, A.B.; Gomes, C.C.; Gonçalves, M.R.F.; Delucis, R.A. Thermally Treated Granite Slurry Waste as a Mitigating Agent for Sisal Fiber Mineralization in Fiber-cement Composites. *Int. J. Appl. Ceram. Technol.* **2025**, *22*, e15157. [CrossRef]
5. Insaurriaga, G.L.; Gomes, C.C.; Ribeiro, F.V.; Calegaro, G.L.; Silveira, T.A.; Cruz, L.F.; Cruz, J.A.; Amico, S.C.; Delucis, R.A. Effect of Hybridization of Carbon Fibers on Mechanical Properties of Cellulose Fiber–Cement Composites: A Response Surface Methodology Study. *C* **2024**, *10*, 41. [CrossRef]
6. Hosseinpourpia, R.; Varshoee, A.; Soltani, M.; Hosseini, P.; Ziaei Tabari, H. Production of Waste Bio-Fiber Cement-Based Composites Reinforced with Nano-SiO_2 Particles as a Substitute for Asbestos Cement Composites. *Constr. Build. Mater.* **2012**, *31*, 105–111. [CrossRef]
7. Ardanuy, M.; Claramunt, J.; Toledo Filho, R.D. Cellulosic Fiber Reinforced Cement-Based Composites: A Review of Recent Research. *Constr. Build. Mater.* **2015**, *79*, 115–128. [CrossRef]
8. Hasan, K.M.F.; Horváth, P.G.; Alpár, T. Lignocellulosic Fiber Cement Compatibility: A State of the Art Review. *J. Nat. Fibers* **2022**, *19*, 5409–5434. [CrossRef]
9. Tolêdo Filho, R.D.; Scrivener, K.; England, G.L.; Ghavami, K. Durability of Alkali-Sensitive Sisal and Coconut Fibres in Cement Mortar Composites. *Cem. Concr. Compos.* **2000**, *22*, 127–143. [CrossRef]
10. Ferreira, S.R.; de Andrade Silva, F.; Lima, P.R.L.; Toledo Filho, R.D. Effect of Hornification on the Structure, Tensile Behavior and Fiber Matrix Bond of Sisal, Jute and Curauá Fiber Cement Based Composite Systems. *Constr. Build. Mater.* **2017**, *139*, 551–561. [CrossRef]
11. Aramburu, A.B.; Rossetto, H.L.; Magalhães, W.L.E.; Trindade, G.H.; de Avila Delucis, R. Cement Matrix Reinforced with Microfibrillated Cellulose Treated with Furfuryl Alcohol. *Cellulose* **2023**, *30*, 10297–10312. [CrossRef]
12. da Silveira, T.A.; Ribeiro, F.V.; Gomes, C.C.; Aramburu, A.B.; Amico, S.C.; Missio, A.L.; Delucis, R.D.A. Synergistic Effects of Furfurylated Natural Fibers and Nanoclays on the Properties of Fiber–Cement Composites. *Ceramics* **2025**, *8*, 68. [CrossRef]
13. Wei, J.; Meyer, C. Utilization of Rice Husk Ash in Green Natural Fiber-Reinforced Cement Composites: Mitigating Degradation of Sisal Fiber. *Cem. Concr. Res.* **2016**, *81*, 94–111. [CrossRef]
14. Da Silva, E.J.; Marques, M.L.; Velasco, F.G.; Fornari Junior, C.; Luzardo, F.M.; Tashima, M.M. A New Treatment for Coconut Fibers to Improve the Properties of Cement-Based Composites—Combined Effect of Natural Latex/Pozzolanic Materials. *Sustain. Mater. Technol.* **2017**, *12*, 44–51. [CrossRef]
15. Tonoli, G.H.D.; Santos, S.F.; Joaquim, A.P.; Savastano, H. Effect of Accelerated Carbonation on Cementitious Roofing Tiles Reinforced with Lignocellulosic Fibre. *Constr. Build. Mater.* **2010**, *24*, 193–201. [CrossRef]
16. Bencardino, F.; Mazzuca, P.; do Carmo, R.; Costa, H.; Curto, R. Cement-Based Mortars with Waste Paper Sludge-Derived Cellulose Fibers for Building Applications. *Fibers* **2024**, *12*, 13. [CrossRef]

17. Hauser, A.; Eggenberger, U.; Peters, T. Origin and Characterisation of Fly Ashes from Cellulose Industries Containing High Proportions of Free Lime and Anhydrite. *Cem. Concr. Res.* **1999**, *29*, 1569–1573. [CrossRef]
18. Wang, Y.; He, B.; Zhao, L.; Zhao, G. Synergetic Effect of Cationic Polymers on Water Repellency of Cellulosic Fiber Network Paper Filled with Waste Lime Sludge. *J. Residuals Sci. Technol.* **2017**, *14*, 19–25. [CrossRef]
19. *NBR NM 76*; Portland Cement: Determination of Fineness by the Air Permeability Method (Blaine Method). Brazilian Association of Technical Standards (ABNT): Rio de Janeiro, Brazil, 1996. (In Portuguese)
20. *NBR NM 65*; Portland Cement: Determination of Setting Times. Brazilian Association of Technical Standards (ABNT): Rio de Janeiro, Brazil, 2002. (In Portuguese)
21. *ABNT NBR: 5743*; Cimento Portland—Determinação de Perda Ao Fogo. Brazilian Association of Technical Standards (ABNT): Rio de Janeiro, Brazil, 1989.
22. *ABNT NBR: 9203*; Cimento Portland Comum e Clínquer—Análise Química Por Complexometria. Brazilian Association of Technical Standards (ABNT): Rio de Janeiro, Brazil, 2004.
23. *ABNT NBR: 5745*; Cimento Porland—Determinação de Anidrido Sulfúrico. Brazilian Association of Technical Standards (ABNT): Rio de Janeiro, Brazil, 1989.
24. *ASTM C305-20*; Practice for Mechanical Mixing of Hydraulic Cement Pastes and Mortars of Plastic Consistency. ASTM International: Washington, DC, USA, 2020.
25. *ASTM C348*; Flexural Strength of Hydraulic-Cement Mortars. ASTM International: Washington, DC, USA, 2002.
26. *ASTM C948*; Standart Test Method for Dry and Wet Bulk Density, Water Absorption, and Apparent Porosity of Thin Sections of Glass-Fiber Reinforced Concrete. ASTM International: Washington, DC, USA, 2023.
27. León-Martínez, F.M.; Cano-Barrita, P.F.d.J.; Castellanos, F.; Luna-Vicente, K.B.; Ramírez-Arellanes, S.; Gómez-Yáñez, C. Carbonation of High-Calcium Lime Mortars Containing Cactus Mucilage as Additive: A Spectroscopic Approach. *J. Mater. Sci.* **2021**, *56*, 3778–3789. [CrossRef]
28. dos Santos, V.; Tonoli, G.H.D.; Mármol, G.; Savastano, H. Fiber-Cement Composites Hydrated with Carbonated Water: Effect on Physical-Mechanical Properties. *Cem. Concr. Res.* **2019**, *124*, 105812. [CrossRef]
29. Ballesteros, J.E.M.; Mármol, G.; Filomeno, R.; Rodier, L.; Savastano, H.; Fiorelli, J. Synergic Effect of Fiber and Matrix Treatments for Vegetable Fiber Reinforced Cement of Improved Performance. *Constr. Build. Mater.* **2019**, *205*, 52–60. [CrossRef]
30. Wei, J.; Meyer, C. Degradation Rate of Natural Fiber in Cement Composites Exposed to Various Accelerated Aging Environment Conditions. *Corros. Sci.* **2014**, *88*, 118–132. [CrossRef]
31. Azevedo, A.G.S.; Savastano, H. Assessment of Carbonation as a Complementary Strategy to Increase the Durability of Magnesium Oxysulfate (MOS)-Based Fiber Cement Boards. *Constr. Build. Mater.* **2024**, *438*, 137086. [CrossRef]
32. Hou, M.; Li, Z.; Li, V.C. Green and Durable Engineered Cementitious Composites (GD-ECC) with Recycled PE Fiber, Desert Sand, and Carbonation Curing: Mixture Design, Durability Performance, and Life-Cycle Analysis. *Constr. Build. Mater.* **2024**, *414*, 134984. [CrossRef]
33. Neves Junior, A.; Ferreira, S.R.; Toledo Filho, R.D.; Fairbairn, E.d.M.R.; Dweck, J. Effect of Early Age Curing Carbonation on the Mechanical Properties and Durability of High Initial Strength Portland Cement and Lime-Pozolan Composites Reinforced with Long Sisal Fibres. *Compos. Part. B Eng.* **2019**, *163*, 351–362. [CrossRef]
34. Cabral, M.R.; Nakanishi, E.Y.; Fiorelli, J. Evaluation of the Effect of Accelerated Carbonation in Cement–Bagasse Panels after Cycles of Wetting and Drying. *J. Mater. Civ. Eng.* **2017**, *29*, 04017018. [CrossRef]
35. Lima, P.R.L.; Santos, H.M.; Camilloto, G.P.; Cruz, R.S. Effect of Surface Biopolymeric Treatment on Sisal Fiber Properties and Fiber-Cement Bond. *J. Eng. Fibers Fabr.* **2017**, *12*, 59–71. [CrossRef]
36. Biskri, Y.; Babouri, L.; Boukhelf, F.; Charradi, K.; Annaba, K.; El Mendili, Y. On the Physical-Mechanical Behavior of Fiber Cement Composite: Effect of Chemical Treatment of Sisal Fibers. *J. Build. Eng.* **2025**, *101*, 111978. [CrossRef]